Science of the Total Environment 855 (2023) 158634

Contents lists available at ScienceDirect

Science of the Total Environment

journal homepage: www.elsevier.com/locate/scitotenv

Potential health and economic impacts of shifting manufacturing from China to Indonesia or India

Qi Ran [a,b], Shao-Yi Lee [b], Duofan Zheng [a,b], Han Chen [a,g], Shili Yang [c], John C. Moore [d,e,f], Wenjie Dong [a,b,*]

[a] School of Atmospheric Sciences, Key Laboratory of Tropical Atmosphere-Ocean System, Ministry of Education, Sun Yat-sen University, Zhuhai 519082, China
[b] Southern Marine Science and Engineering Guangdong Laboratory (Zhuhai), Zhuhai 519082, China
[c] Beijing Meteorological Observation Centre, Beijing Meteorological Bureau, Beijing 100089, China
[d] College of Global Change and Earth System Science, Beijing Normal University, Beijing 100875, China
[e] Arctic Centre, University of Lapland, Rovaniemi 96101, Finland
[f] CAS Center for Excellence in Tibetan Plateau Earth Sciences, Beijing 100101, China
[g] Central-South Architectural Design Institute Co.,Ltd., Wuhan 430064

HIGHLIGHTS

- $PM_{2.5}$ responses to idealized scenarios reflecting manufacturing shifts were simulated.
- Significant changes in $PM_{2.5}$-related mortality and economic cost occurred over Asia.
- Third countries without GDP rise could see mortality rise and may demand compensation.

GRAPHICAL ABSTRACT

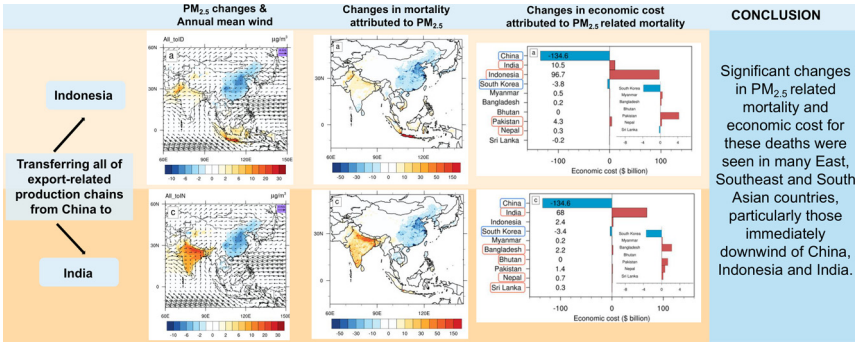

ARTICLE INFO

Editor: Jay Gan

Keywords:
Manufacturing shifts
$PM_{2.5}$-related mortality
Economic cost
Earth system model

ABSTRACT

The diversification or decoupling of production chains from China to alternative Asian countries such as India or Indonesia would impact the spatial distribution of anthropogenic emissions, with corresponding economic impacts due to mortality associated with particulate matter exposure. We evaluated these changes using the Community Earth System Model, the Integrated Exposure-Response (IER) model and Willingness To Pay (WTP) method. Significant effects on $PM_{2.5}$ related mortality and economic cost for these deaths were seen in many East, Southeast and South Asian countries, particularly those immediately downwind of these three countries. Transferring all of export-related manufacturing to Indonesia resulted in significant mortality decreases in China and South Korea by 78k (5 per 100k) and 1k (2 per 100k) respectively, while Indonesia's mortality significantly increased (73.7k; 29 per 100k), as well as India, Pakistan and Nepal. When production was transferred to India, mortality rates in East Asia show similar changes to the Indonesian scenario, while mortalities in India increased dramatically (87.9k; 6 per 100k), and mortalities in many neighbors of India were also severely increased. Nevertheless, the economic costs for $PM_{2.5}$ related mortality were much smaller than national GDP changes in China (0.9 % of GDP vs. 18.3 % of GDP), India (2.7 % of GDP vs. 84.3 % of GDP) or Indonesia (9.4 % of GDP vs. 337 % of GDP) due to shifting all of export-related production lines from China to India or Indonesia. Morally, part of the benefits of economic activity should be used to compensate the neighboring communities where mortality increases occur.

* Corresponding author at: Southern Marine Science and Engineering Guangdong Laboratory (Zhuhai), Zhuhai 519000, China.
E-mail address: dongwj3@mail.sysu.edu.cn (W. Dong).

http://dx.doi.org/10.1016/j.scitotenv.2022.158634
Received 21 June 2022; Received in revised form 5 September 2022; Accepted 5 September 2022
Available online 8 September 2022

1. Introduction

The ongoing coronavirus COVID-19 has disrupted global supply, demand and logistics infrastructure (Guan et al., 2020; Ivanov, 2020; Nicola et al., 2020); countries with greater dependency on foreign supply chains have been more negatively affected (Fernandes, 2020). 94 % of the Fortune 1000 companies have suffered from interrupted supply chains caused by COVID-19 outbreaks (Sherman, 2020). The resulting material shortages and delivery delays have reduced production, and many multinational businesses have reconsidered their manufacturing deployments (Hayakawa and Mukunoki, 2021; Liu et al., 2020; Free and Hecimovic, 2021). During recent decades, many international companies have become greatly dependent on Chinese production and supplies, which has increased instability and uncertainties in global trade and supply chains during the COVID-19 pandemic. On July 17, 2020, the Japanese Ministry of Economy, Trade and Industry announced that a first batch of 87 Japanese companies had transferred portions of their supply chain in China to Southeast Asia or back to Japan to reduce the dependence on China. Southeast Asian countries with relatively low labor costs, such as Vietnam, Indonesia and India, are probably the most likely to benefit from a shift of global manufacturing (Lin and Lanng, 2020). In fact, the reshaping of global manufacturing is not only related to epidemic outbreaks, but also the rising risk of trade wars, upward trends in nationalism and protectionism, considerations about sustainability and tackling climate change (Hedwall, 2020; Free and Hecimovic, 2021).

Many studies have shown that millions of people worldwide die every year from diseases attributed to long-term exposures to fine particulate matter, particularly $PM_{2.5}$ (Brauer et al., 2016; Burnett et al., 2014; Apte et al., 2015; Wang et al., 2018). International trade activities are associated with emissions of air pollutants. Lin et al. (2014, 2016) calculated emissions embodied in export (EEE) of different regions worldwide and analyzed their impacts on atmospheric environment and human health. Zhang et al. (2017) used global emissions, chemistry, trade and exposure models to estimate premature mortality related to $PM_{2.5}$ pollution from the production and consumption process to show that the health impacts of $PM_{2.5}$ attributable to international trade are significant.

As aerosols will be emitted during the production process, the redistribution of production lines is expected to affect the distribution of aerosol emissions. Abrupt reductions in the emission of aerosols and aerosol precursors due to a socio-economic crisis results in immediate and significant global and regional climate responses, while the effects of CO_2 emission reductions are much smaller in the short term (Ran et al., 2021). Other studies have also found that atmospheric CO_2 concentration and its impact on climate due to carbon transfer are very small and lie within observed interannual variability (Wei et al., 2016; Lin et al., 2016). Hence in our simulations, we only change aerosol and aerosol-precursor emissions. The scenarios used simulate moving half, or all, export-related manufacturing from China to either Indonesia or India.

We explore the potential risks and benefits to human health and social economy of reshaping global manufacturing, via a series of sensitivity experiments using an earth system model (ESM). We redistributed anthropogenic emissions of aerosols and their precursors from the industry, energy and transportation sectors to represent manufacturing shift from China to Indonesia or India and use these emissions within the ESM to determine changes in surface $PM_{2.5}$. India and Indonesia are chosen as the destinations for manufacturing shift due to their relatively large population and territorial area among South and Southeast Asian countries. Indonesia has a maritime setting along the equator, while India is much more continental, which greatly affects the redistribution of aerosols. We then consider $PM_{2.5}$ related mortality from five major diseases, and a widely used metric to monetize attributable mortality and assess economic aspects of transferring manufacturing.

2. Methods

2.1. Model

A baseline and four sensitivity simulations were done with the Community Earth System Model version 1.2.2 (Hurrell et al., 2013). The baseline experiment was the B_2000_CAM5_CN component set, including the Community Atmosphere Model 5 (CAM5) (Neale et al., 2012), Parallel Ocean Program version 2 (POP2), Community Land Surface Model (CLM) version 4.0, the Los Alamos sea ice model (CICE) version 4, all coupled together using the CESM coupler CPL7. The horizontal resolution of CAM5 and CLM was $0.9^\circ \times 1.25^\circ$ latitude-longitude (f09 grid), while that of POP2 and CICE was about 1° (g1v6 grid). The vertical coordinate of CAM5 was a hybrid sigma-pressure system consisting of 30 vertical levels, with model top at about 3.6 hPa. CLM had 15 soil layers to 35 m depth, POP2 had 60 height layers, and CICE had five thickness categories.

The simulations were run with the Modal Aerosol Module with three modes (MAM3). An alternative and more sophisticated seven mode version (MAM7) has been shown to be generally well reproduced by MAM3 (Liu et al., 2012), and so we use the default MAM3 option in B_2000_CAM5_CN. Emissions were based on AeroCom (Aerosol Comparisons between Observations and Models; Textor et al., 2005), although ammonia was prescribed by sulfate in the simplified chemistry of MAM3. Anthropogenic primary black carbon (BC), primary organic matter (POM), sulfur dioxide (SO_2), primary sulfate aerosol and semi-volatile organic gas species (SOAG) were emitted in seven sectors – agriculture, waste, domestic, energy, industry, transportation, shipping.

2.2. Experiment design

The default CESM experiment "B_2000_CAM5_CN" with greenhouse gas (GHG) levels and aerosol emissions of the year 2000 was adjusted to create our "B_2020_CAM5_CN" baseline experiment. The atmospheric GHGs concentrations were updated to that of year 2020 based on NOAA (available at https://gml.noaa.gov/ccgg/trends/). The aerosol emissions were replaced with year 2020 values from the Representative Concentration Pathway 6.0 (RCP6.0) scenario experiment in CESM. The RCP6.0 was created for the 5th Climate Model Intercomparison Project (CMIP5) (Taylor et al., 2012), as an intermediate stabilization emission scenario leading to 6.0 Wm^{-2} increase in radiative forcing by the end of the century (Moss et al., 2010). Since there is no significant difference in emissions and temperatures under any scenario around 2020 (Ran et al., 2021; IPCC, 2014), the choice of RCP scenario is not important in our simulations. The "B_2020_CAM5_CN" was run for 200 years to reach the climate equilibrium state of 2020 (Fig. S1.1), and the following analysis for simulation results was based on the median climate state for the third 100 years.

We redistributed anthropogenic BC, POM, SO_2, primary sulfate aerosol and SOAG emissions in the industry, energy, and transportation sectors to represent manufacturing shifts from China to Indonesia or India. Emissions Embodied in Exports (EEE) was calculated using an Input-output Model (Lin et al., 2016) to determine the proportion of emission transfer in the industry, energy and transportation sectors of China. We integrated the emission sectors described by National Bureau of Statistics of China (NBSC) to meet the classification of emission sectors in CESM (see Table S1). The input-output table for 2017 was used because it is the latest available (NBSC, 2017). The total merchandise exports and imports in China changed little between 2017 and 2020 (Fig. S1.2). Other economic data needed for the calculation was also derived from NBSC. Results show that EEE of China in industry, energy, and transport sector accounts for about 22.4 %, 17.9 % and 23.8 % of total emissions, respectively.

We created four sensitivity simulations for detecting a response of the climate system to manufacturing redistributions based on the climatic equilibrium state of the baseline experiment (Table 1). These are, i) All_toID: all of China EEE transferred to Indonesia; ii) Half_toID: half of China EEE transferred to Indonesia; iii) All_toIN: all of China EEE transferred to India; iv) Half_toIN: half of China EEE of transferred to India. Available labor is generally proportional to population density, so we distributed the EEE of China around Indonesia or India based on the geographic population distribution in 2020 (Fig. S1.3) rather than evenly increasing emissions across Indonesia or India (Fig. 1).

Table 1
Emission scenarios of the baseline experiment and the four sensitivity simulations.

Experiment	Simulated time	Aerosol emissions	GHGs concentration
Baseline experiment	300 years	Same as the emission level of 2020 in RCP6.0	From NOAA ESRL data in 2019
Transferred to Indonesia by 50 % (Half_toID)	100 years (restarted from the 200th year of the baseline)	Same as the emission level of the baseline but 50 % of EEE of China transferred to Indonesia	Same as the baseline
Transferred to Indonesia by 100 % (All_toID)	100 years (restarted from the 200th year of the baseline)	Same as the emission level of the baseline but 100 % EEE of China transferred to Indonesia	Same as the baseline
Transferred to India by 50 % (Half_toIN)	100 years (restarted from the 200th year of the baseline)	Same as the emission level of the baseline but 50 % of EEE of China transferred to Indonesia	Same as the baseline
Transferred to India by 100 % (All_toIN)	100 years (restarted from the 200th year of the baseline)	Same as the emission level of the baseline but 100 % EEE of China transferred to Indonesia	Same as the baseline

2.3. Correction for modeled $PM_{2.5}$

We compared the simulated 100-year mean $PM_{2.5}$ concentrations in our baseline run with $PM_{2.5}$ concentrations for 2010–2020 at 0.1° × 0.1° horizontal resolution given by van Donkelaar et al. (2021) of combined satellite observations, chemical transport modeling and ground-based monitoring. The distribution of $PM_{2.5}$ concentrations in the baseline was similar to that of the satellite-derived $PM_{2.5}$ (van Donkelaar et al., 2021), but with significant differences in some areas of interest in this study (China, India and Indonesia), and further afield over West Asia and North Africa (Fig. S2.1). Since ammonia is not directly simulated in the MAM3 aerosol module, ammonium sulfate is effectively prescribed. We performed the baseline experiment with the computationally more expensive MAM7 module for year 2000, which explicitly simulated ammonia, and improved $PM_{2.5}$ concentrations over the Indian subcontinent and North China, but not over Indonesia and Southeast Asia (Fig. S2.2). Therefore, we do not consider the use of MAM3 rather than MAM7 as the main reason for the $PM_{2.5}$ deficiencies.

The multi-year average surface concentrations of each simulated aerosol (with diameters <2.5 μm) in the baseline have similar spatial distribution as the 2010–2020 average from Modern-Era Retrospective analysis

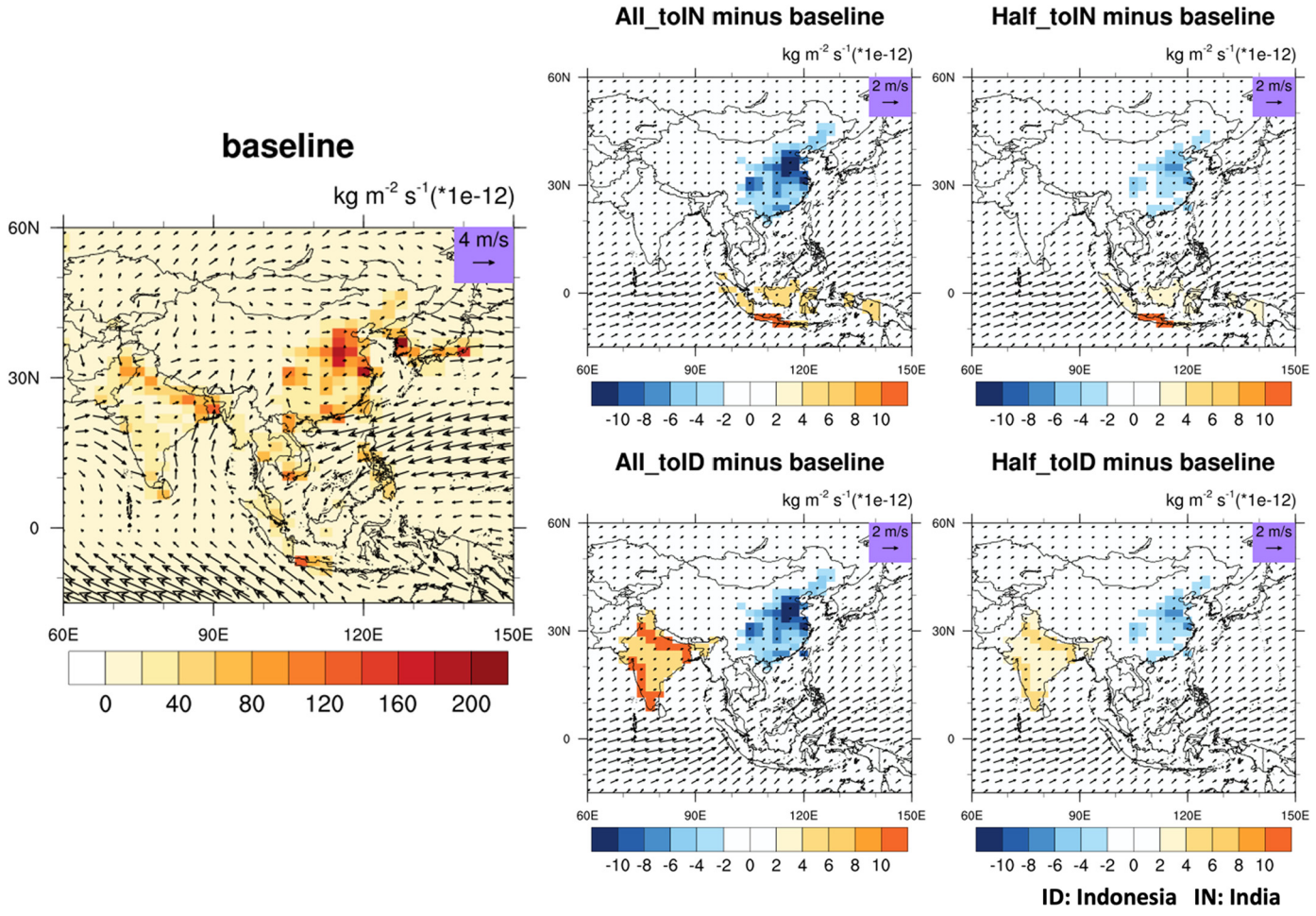

Fig. 1. Annual mean total anthropogenic aerosol and aerosol precursor emissions (10^{-12} kg m^{-2} s^{-1}) for the baseline for the year 2020, and the differences in emissions between the four sensitivity simulations and the baseline. Here is the hypothetical aerosol mass emission, described as the sum of BC, POM, primary sulfate aerosol, sulfate and SOA emission. Sulfate and SOA here refer to the part of SO_2 and SOAG that has been converted to sulfate or SOA. The arrows in the baseline panel are the median value of the 100-year annual mean surface (the lowest level of the model) wind (0.9° × 1.25°) in the baseline, and the standard deviation of 100-year annual mean surface wind in the sensitivity simulations are shown in the four panels for emission differences.

for Research and Applications version 2 (MERRA-2; GMAO, 2015; Fig. S2.3). However, sulfate and POM in the baseline were significantly underestimated across much of Asia, particularly North India, East China and the island of Java. The most plausible reason is that the emission inventory used by MAM3 did not capture the high emissions of anthropogenic sulfur dioxide and organic carbon emissions in regions where sulfate and POM were severely underestimated. Sea salt and dust showed some differences, but are not affected by transfer of manufacturing (Figs. S2.4 and S2.5). In fact, the $PM_{2.5}$ bias outside East Asia, South Asia and Southeast Asia, had little effect on our results, as $PM_{2.5}$ concentrations and $PM_{2.5}$ related mortality outside Asia did not change significantly in our simulations (Figs. S3.1 and S3.2).

Because of the health impacts of $PM_{2.5}$ scale non-linearly with concentration – that is the same increase in concentration has larger impacts when added to a low concentration background than it does on a high concentration one, we need to correct simulated $PM_{2.5}$ in Asia with reanalysis data and observed data. Firstly, we corrected modeled sulfate, BC, POM, dust and sea salt aerosol concentrations (only considering aerosols <2.5 μm in diameter) in Asia, by multiplying them by the ratio of each aerosol concentration in MERRA-2 to that in the baseline (0.9° × 1.25°; Fig. S2.3). The weighted sum of the five aerosols and secondary organic aerosol (SOA) represents the simulated $PM_{2.5}$ concentration (Eq. (1)). The weight for each aerosol was found by multiple linear regression (MLR) between aerosols and the satellite-derived $PM_{2.5}$ from van Donkelaar et al. (2021). Particular aerosols in various countries are highly correlated (we took $R > 0.85$ here; Sheet 1 in Supplementary tables 1), so, for that country we combined the highly correlated aerosols into a single variable (Highlights in Supplementary tables 1) for the MLR to avoid issues with overfitting. The same procedure was applied for $PM_{2.5}$ in all experiments, and the subsequent calculations and analysis are based on the corrected $PM_{2.5}$ concentrations.

$$PM_{2.5,i(r)} = \Sigma_{g=1}^{6} Aerosol_{g,i(r)} \times W_{g,r} \quad (1)$$

Here, $PM_{2.5,\,i(r)}$ is the corrected $PM_{2.5}$ concentration of grid cell i located in Asian country r. $Aerosol_{g,i(r)}$ represents the concentration of Aerosol g corrected by MERRA-2 data. $W_{g,r}$ is the regression coefficient for aerosol g in country r.

The corrected spatial distribution of 100-year mean surface $PM_{2.5}$ concentrations in the baseline simulation is compared with 2010–2020 mean satellite-derived $PM_{2.5}$ (van Donkelaar et al., 2021) in Fig. 2. The high emissions in the North China and the Indo-Gangetic plains were well reproduced. Corrected regional mean $PM_{2.5}$ concentrations of most Asian countries were within 20 % of observations (van Donkelaar et al., 2021), and within the 95 % confidence intervals of the medians (Supplementary tables 2). Despite clear differences in some places we consider that baseline simulation satisfactorily reproduced the mean present surface $PM_{2.5}$ concentrations and can be used to estimate related mortality and economic costs in our hypothetical cases.

2.4. Calculation of $PM_{2.5}$ related mortality

We considered the five major disease endpoints of $PM_{2.5}$ related mortality where surface $PM_{2.5}$ concentrations are considered a risk factor in the Global Burden of Disease (GBD) 2010 (Global Burden of Disease Collaborative Network, 2013). For adults (age ≥ 25), these endpoints are ischemic heart disease, cerebrovascular disease (stroke), chronic obstructive pulmonary disease, and lung cancer, and for children under 5, acute respiratory lung infection.

2.4.1. Input data

2.4.1.1. Global $PM_{2.5}$ and population surfaces. We simulated global annual-average ambient $PM_{2.5}$ concentrations at 1° grid resolution using CESM 1.2.2. We used the global 30 km gridded population data set (Center for International Earth Science Information Network - CIESIN - Columbia University, 2018) of 2020 population in our mortality model, with the $PM_{2.5}$ concentrations interpolated to the same grid using areal conservative remapping.

2.4.1.2. Mortality data. We obtained the cause-specific mortalities for the five endpoints in 2019 from the GBD (2019) - the most recent publicly available data set at the Institute for Health Metrics and Evaluation (IHME). Deaths per 100,000 population in 2019 for the five endpoints in 54 countries and three regions are provided in the Supplementary tables 3.

2.4.2. The Concentration-Response function

The Concentration-Response (C-R) function is a mathematical equation that describes the relationship between exposures to $PM_{2.5}$ and the relative risk of mortality for each endpoint. Here, we employed the integrated exposure-response functions (IERs) (Burnett et al., 2014) to constrain the shape of the C-R relationship and estimate relative risks attributed to $PM_{2.5}$ exposure for the five endpoints. The IER framework parametrizes the dependence of relative risk, RR, on concentration, C (Burnett et al., 2014):

$$\begin{aligned} RR(C) &= 1 + \alpha\left[1 - \exp\left(-\gamma(C - C_0)^{\delta}\right)\right] \text{ for } C > C_0 \\ RR &= 1 \text{ for } C \le C_0 \end{aligned} \quad (2.1)$$

For each endpoint, C_0 represents a theoretical minimum-risk concentration above which there is evidence indicating health benefits of $PM_{2.5}$ exposure reductions, and parameters α, γ, and δ determine the overall shape of the concentration-response relationship. A distribution of 1000 estimates of these parameters for each endpoint for all ages was provided in GBD 2010 (Global Burden of Disease Collaborative Network, 2013). Here we use the median value of the RR from the 1000-member parameter set found over $PM_{2.5}$ concentrations from 0 to 200 μg/m^3 at 0.1 μg/m^3 steps (see Supplementary tables 4).

2.4.3. Modeling of $PM_{2.5}$ related mortality

We estimated the premature mortality $M_{i(r),k}$ of all ages for disease endpoint k attributable to ambient $PM_{2.5}$ for grid cell i located in region r (see Eq. (2.2)). $\widehat{I}_{r,k}$ represents the hypothetical "underlying incidence" (i.e., cause-specific mortality rate) for endpoint k that would remain for region r if $PM_{2.5}$ concentrations were reduced to the theoretical minimum risk concentration throughout that region.

$$M_{i(r),k} = P_{i(r)} \times \widehat{I}_{r,k} \times \left(RR_k\left(C_{i(r)}\right) - 1\right)/100000 \; where \; \widehat{I}_{r,k} = I_{r,k}/\overline{RR}_{r,k} \quad (2.2)$$

Here, $P_{i(r)}$ is the population of grid cell i located in region r, $I_{r,\,k}$ is the reported regional average annual deaths (per 100,000) for endpoint k in region r, $C_{i(r)}$ represents the annual-average $PM_{2.5}$ concentration in cell i, $RR_k(C_{i(r)})$ is the relative risk for end point k at concentration $C_{i(r)}$, and $\overline{RR}_{r,k}$, as defined below (Eq. (2.3)), represents the average population-weighted relative risk for end point k within region r:

$$\overline{RR}_{r,k} = \frac{\Sigma_{i=1}^{N} P_{i(r)} \times RR_k\left(C_{i(r)}\right)}{\Sigma_{i=1}^{N} P_{i(r)}} \quad (2.3)$$

In addition to the absolute number of premature deaths related to $PM_{2.5}$, we also calculated the per-capita mortality (Eq. (2.4)) to eliminate the influence of population density.

$$\overline{M}_{i(r),k} = \frac{M_{i(r),k} \times 100000}{P_{i(r)}} \quad (2.4)$$

$\overline{M}_{i(r),k}$ is the per-capita attributable mortality for grid cell i located in region r.

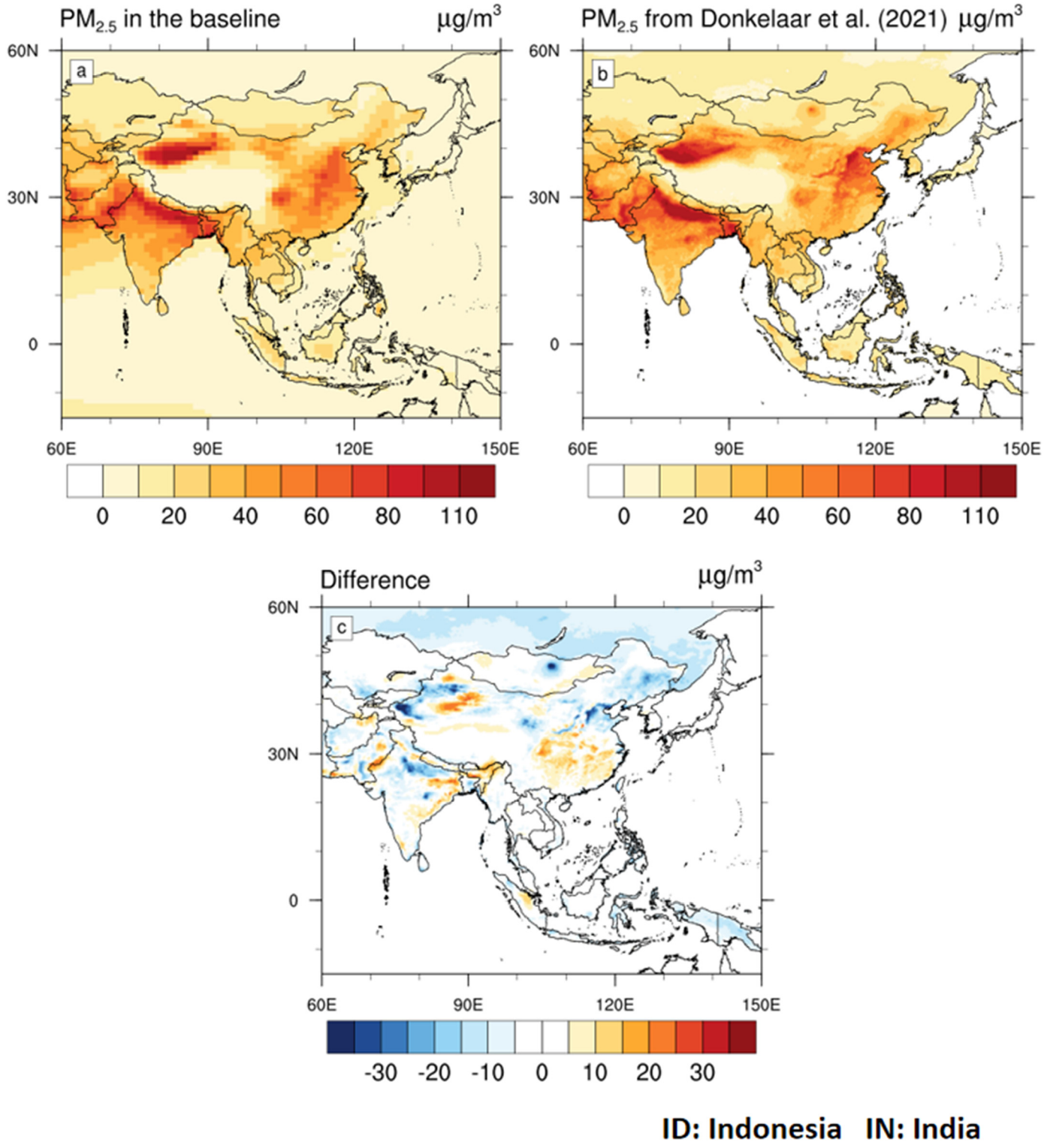

Fig. 2. Multi-year mean surface $PM_{2.5}$ concentrations for (a) the baseline simulation with horizontal resolution 0.9° × 1.25° over the third 100 years (after bias correction), and (b) van Donkelaar et al. (2021) with horizontal resolution 0.1° × 0.1° over 2010–2020. The differences (model- van Donkelaar et al., 2021) between them are shown in (c).

2.5. Economic assessment

2.5.1. Economic cost for mortality

We used the Value of Statistical Life (VSL), the most generally used metric to monetize attributable mortality for $PM_{2.5}$ (OECD, 2012, 2014, 2017; Lu et al., 2017; Giannadaki et al., 2018), to evaluate the economic cost attributed to $PM_{2.5}$ related mortality due to manufacturing transfer. The VSL is the marginal value of a reduction in the risk of dying, and is therefore defined as the rate at which the people are prepared to trade off income for risk reduction (Braathen et al., 2009):

$$VSL = \frac{\partial WTP}{\Delta R} \tag{3.1}$$

where R is the risk of dying and ∂WTP is an individual's "Willingness To Pay" to reduce mortality risk by ΔR. VSL is an integration of individual values for small changes in mortality risk, rather that the value of a certain person's life (OECD, 2012).

We derived the VSL value in constant 2015 USD of PPP (purchasing power parity) terms for the individual countries or regions (OECD Statistics, 2020; see Table S2) for the year 2019 (the latest data available). The estimation of VSL here accounts for differences in income levels and income elasticities across countries. The income elasticity is 0.8, 0.9 and 1 for high-, middle- and low-income countries respectively, indicating that as incomes rise, the WTP for a marginal reduction in the risk of attributable death for $PM_{2.5}$ also rises, but not quite in proportion to the rise in incomes (OECD, 2017). The total economic cost in country/region r for the year Y can be assessed by multiplying the total number of $PM_{2.5}$ related deaths in country/region r $\Sigma_{i=1}^{N} M_{i(r)}$ with the corresponding $VSL_{r,\ Y}$,

$$\text{Economic Cost} = \Sigma_{i=1}^{N} M_{i(r)} \times VSL_{r,Y} \tag{3.2}$$

2.5.2. Economic benefits from additional production

Simple estimation for potential economic changes to Gross Domestic Product (GDP) due to the shift of production lines comes from CO_2 per GDP in China, Indonesia and India (Andrew, 2020; BP, 2020), was found using Eq. (4).

$$\text{Economic benefits} = \Delta E_r / F_r \tag{4}$$

where ΔE_r is the emission change in country r, and F_r refers to CO_2 emissions per GDP in country r.

2.6. Uncertainty and significance test

For each experiment, we calculate yearly mortality rate per 30 × 30 km grid cell based on annual mean $PM_{2.5}$ for 100 years (in the climate equilibrium state), then the 100 estimates for mortality differences between the baseline and sensitivity simulations are calculated for each grid cell and their median values are shown in Fig. 4. For an individual country, we consider the sum of mortality rate in each grid cell as national total mortality rate, then deaths per 100k are calculated as the per-capita mortality of this country. One hundred estimates of national per-capita and total mortality and their changes due to manufacturing shift are calculated for each Asian country, and we use the 2.5 and 97.5 percentiles of the 100 estimates as the ranges of mortality rates and their changes (Supplementary tables 5 and 6). In addition, statements about whether changes in national mortality are significant were evaluated with the non-parametric Wilcoxon signed-rank test for each Asian country (Supplementary tables 5 and 6). The two-tailed test was carried out at the 0.05 significance level.

For 100-year estimates of national total mortality rates, we calculate corresponding attributable economic cost for mortality using Eq. (3.2). Then we use the same method as for mortality to obtain the uncertainty and perform the significance test for economic costs of each Asian country (Supplementary tables 7).

3. Results

3.1. Changes in $PM_{2.5}$ concentrations

As expected, the shift of manufacturing from China to India/Indonesia would result in significant changes in surface $PM_{2.5}$ concentrations in China, India and Indonesia (Fig. 3). When half or all of export-related production lines were transferred to Indonesia, northern China's $PM_{2.5}$ concentrations declined by over 4 μg m^{-3}, with local differences much higher than country means (Table 2). $PM_{2.5}$ declines can be also seen in other East and Southeast Asian countries, such as the Korean Peninsula (All_toID), Thailand, Laos, Cambodia, and Vietnam (Half_toID). Transferring industry to Indonesia raised local $PM_{2.5}$, especially in Java Island with rises over 10 μg m^{-3}, while the country mean increased by about 6.1 or 2.6 μg m^{-3} in scenarios All_toID and Half_toID. $PM_{2.5}$ increases also occurred in Pakistan, North India, Nepal, driven by the consistent changes in annual mean surface winds blowing from Java Island across the equator towards Northern India (Fig. 1). In the rest of the world, $PM_{2.5}$ concentrations were almost constant after the shift of manufacturing, although there were small but consistent changes in $PM_{2.5}$ seen in Africa and Central Australia that hint at possible teleconnections to the deserts there (Fig. S3.1a, b).

Transferring production lines to India had similar impacts on China $PM_{2.5}$ concentrations as with manufacturing shifts to Indonesia (Fig. 3). $PM_{2.5}$ in North Korea and South Korea decreased by around 1 μg m^{-3} in scenario All_toIN. Except for slight $PM_{2.5}$ increases in Myanmar, $PM_{2.5}$ changes were not obvious in most southeast Asian countries. As expected, the most significant increases occurred in the Indo-Gangetic Plain, rising by over 10 μg m^{-3}. $PM_{2.5}$ in countries close to India, such as Pakistan, Nepal, Bhutan and Bangladesh were also affected by the manufacturing shift to India. $PM_{2.5}$ concentrations in other parts of the world were barely affected (Fig. S3.1c, d). The impacts of manufacturing shift on surface $PM_{2.5}$ concentrations were localized to East, South and Southeast Asia because aerosol and aerosol precursor emissions were from the surface and not well-mixed in the whole atmosphere, or even the troposphere. So, shifting manufacturing would affect $PM_{2.5}$ concentrations in countries whose emissions had changed and in their downwind countries.

3.2. Attributable mortality for $PM_{2.5}$

We use the abbreviations m for millions and k for thousands of deaths per year. Attributable mortality for $PM_{2.5}$ in the baseline and the four sensitivity experiments was estimated based on IERs (Burnett et al., 2014), (Eq. (2)). Giannadaki et al. (2016) applied IERs to evaluate attributable premature mortality for annual mean $PM_{2.5}$ in 2010. They attributed 3.15 m deaths globally in 2010, with China accounting for 1.33 m, followed by India with 575k. China's attributable mortality for $PM_{2.5}$ in 2016 estimated by Maji et al. (2018) was 0.96 m (with a 95 % confidence interval of 0.45 to 1.36 m; we use 2.5 %–97.5 % percentiles as the ranges), accounting for 10.0 % of total reported deaths in China. We estimate $PM_{2.5}$ related mortality in China, India and Indonesia in the baseline at 1.66 m (1.60–1.73 m), 0.99 m (0.92–1.07 m) and 78k (49–163k; Supplementary tables 5) respectively. In most of the regions where $PM_{2.5}$ simulation bias is corrected, our estimates are comparable to other estimations (OECD Statistics, 2020). China's mortality rate is overestimated by 16 %, India's by 1 %, and Indonesia's underestimated by 27 % (OECD Statistics, 2020; Supplementary tables 5).

Since attributable mortality for $PM_{2.5}$ depends on the population density (which is unchanged by design in these sensitivity experiments), and $PM_{2.5}$ concentrations (Eq. (2.2)), its spatial change is similar to changes in surface $PM_{2.5}$ concentrations (Fig. S3.1 vs. Fig. S3.2; Fig. 3 vs. Fig. 4). Outside East, Southeast and South Asia there are only insignificant changes in attributable mortality due to the manufacturing shifts (Figs. 4, S3.2).

Transferring all of export-related production lines into Indonesia (scenario All_toID) resulted in more significant mortality changes over Asia, compared with scenario Half_toID (Fig. 4a vs. b). China's per-capita mortality attributed to $PM_{2.5}$ decreased dramatically by around 5 deaths per 100k and total mortality by 78k, with the largest decline in North China, while they dropped by 3 per 100k and 46.9k in total under the Half_toID simulation. Significant declines in per-capita and total mortality can also be seen in South Korea, by 2 per 100k and 1k in total in the All_toID simulation, and by 1 per 100k and 0.4k in the Half_toID simulation. In the All_toID, mortality reductions can be seen in North Korea and Southern Japan (Fig. 4a), while national total deaths of the two countries changed insignificantly at 0.05 significance level. More modest and less significant declines are simulated in East Asian counties in the Half_toID simulation (see Supplementary tables 5). In both Half_toID and All_toID scenarios, mortality increased most in Indonesia and with similar patterns, with per-capita and total mortality rising by 29 per 100k and 73.7k, and by 17 per 100k and

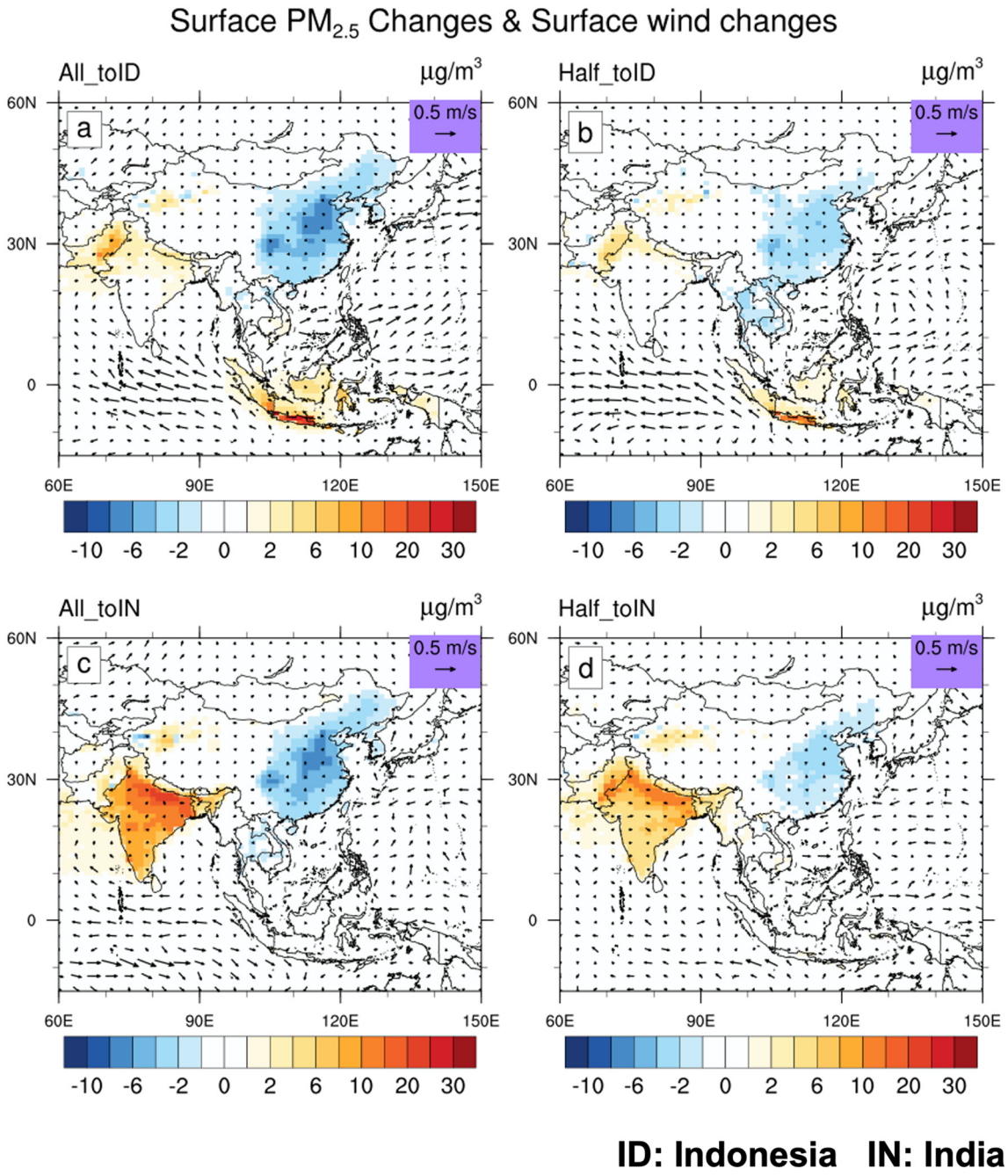

Fig. 3. The median value of the 100-year changes in annual mean surface $PM_{2.5}$ concentrations (0.9° × 1.25°, color bar) and that in annual mean surface (the lowest level of the model) wind (0.9° × 1.25°, arrows) in the (a) Half_toID, (b) All_toID, (c) Half_toIN, and (d) All_toIN simulations compared with the baseline experiment.

43.6k respectively. In the wider Southeast Asia region, there were less obvious changes in mortality. Mortality rates in the Indo-Gangetic Plain rose significantly in India (by 1 per 100k or 13.6k), Pakistan (by 3 per 100k or 7.3k) and Nepal (by 2 per 100k or 0.9k) in the All_toID simulation. However, mortality rates in South Asia showed insignificant changes in the Half_toID simulation.

When all or half of the production lines were transferred to India (All_toIN and Half_toIN scenario), changes in attributable mortality for

Table 2
The median value of 100-year regional mean $PM_{2.5}$ concentrations in the baseline at (0.9° × 1.25°) resolution, and the four sensitivity experiments (after bias correction) for China, India and Indonesia. The numbers in parentheses show the 2.5 % and 97.5 % percentiles of the distribution of 100-year regional mean $PM_{2.5}$ concentrations. Unit: μg m^{-3}.

	RCP6.0	Half_toID	All_toID	Half_toIN	All_toIN
China	29.9 (27.6–32.8)	29.1 (26.3–31.8)	28.5 (25.6–31.0)	29.4 (26.8–31.5)	28.5 (26.2–31.1)
India	46.3 (41.1–55.3)	47.1 (40.9–55.3)	47.5 (41.5–63.4)	53.4 (46.7–69.8)	56.8 (50.3–68.1)
Indonesia	13.3 (9.9–30.9)	15.9 (12.6–41.7)	19.4 (14.2–47.1)	14.2 (10.3–35.2)	13.7 (10.4–37.5)

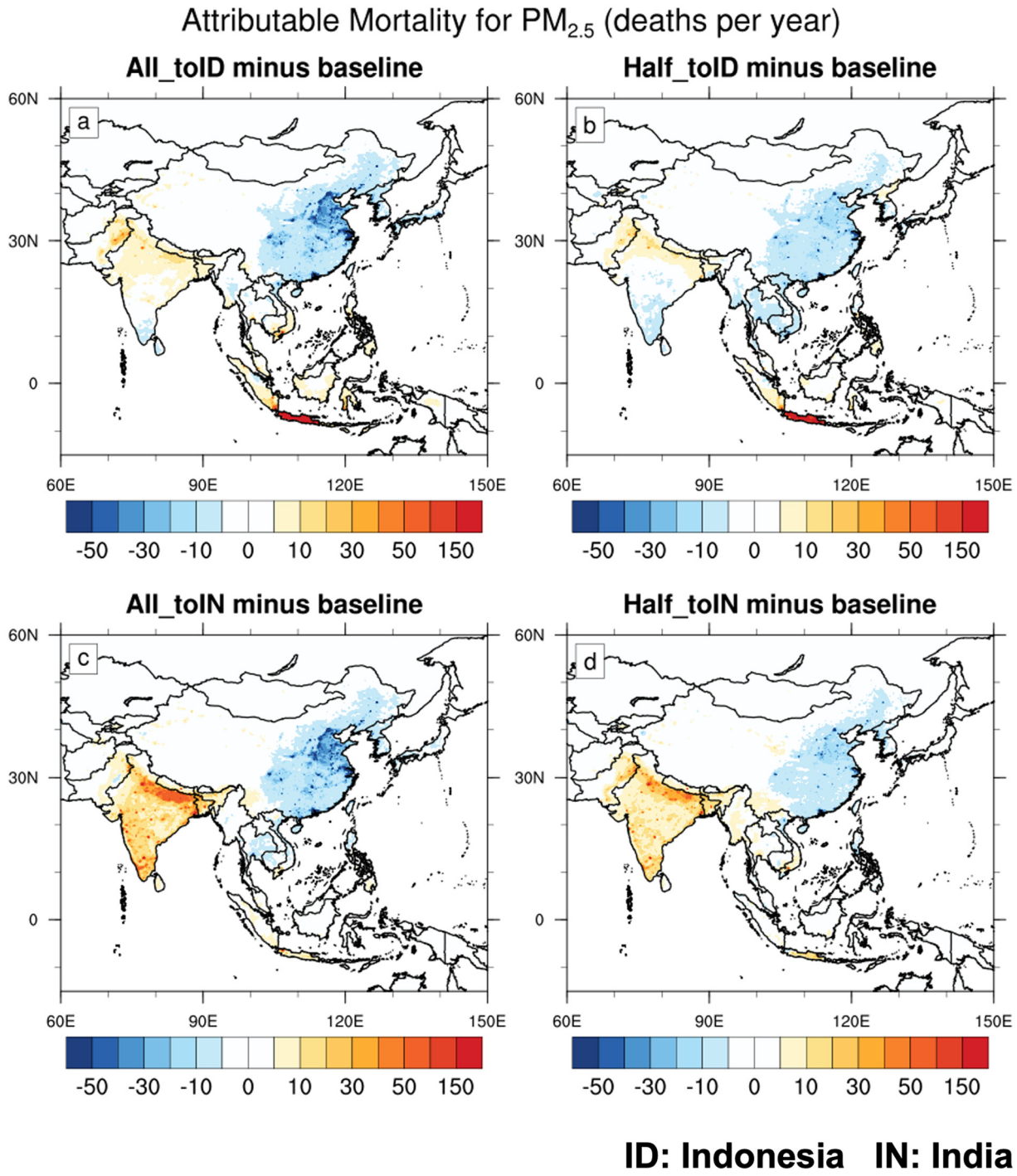

Fig. 4. The median of 100-year estimates of differences of attributable mortality rate per 30 × 30 km grid cell for annual mean surface $PM_{2.5}$ between the four sensitivity simulations and the baseline.

$PM_{2.5}$ in East Asia were quite similar to the Indonesian scenario (Fig. 4). Significant decreases in mortality rate were simulated for China and South Korea (Fig. 5c and d). However, in the Half_toID simulation, the declines in China's mortality rates were smaller than that in Half_toIN, and slight increases can be seen in Yunnan Provence, China. In Southeast Asia, increases in mortality rates can be seen in Indonesia, especially in Java, but national per-capita and total mortality were unchanged at the 0.05 significance level, except for mortality rate of Myanmar which showed significant increase in the Half_toIN scenario. For India, especially over the Gangetic Plain and the southern tip of the India Peninsula, there would be significant increases, with per-capita and total mortality rates increasing by 6 per 100k and 87.9k under the All_toIN scenario, and by 4 per 100k and 57.8k under Half_toIN. National per-capita and total mortality rates of other South Asian countries were also severely affected in the simulations, with rises under All_toIN for Bangladesh by 2 per 100k and 3.9k, Bhutan by 3 per 100k and 0.04k, Nepal by 5 per 100k and 1.9k, and Sri Lanka by 1 per 100k and 0.2k. Pakistan's mortality rate rose under Half_toIN (3 per 100k; 6.4k), while changes were not significant under the All_toIN scenario.

In conclusion, significant changes in attributable mortality for $PM_{2.5}$ occurred in the three countries whose industries were changed in the simulations. Moreover, many countries downwind also experience significant changes in mortality rates. The differences in significance between All

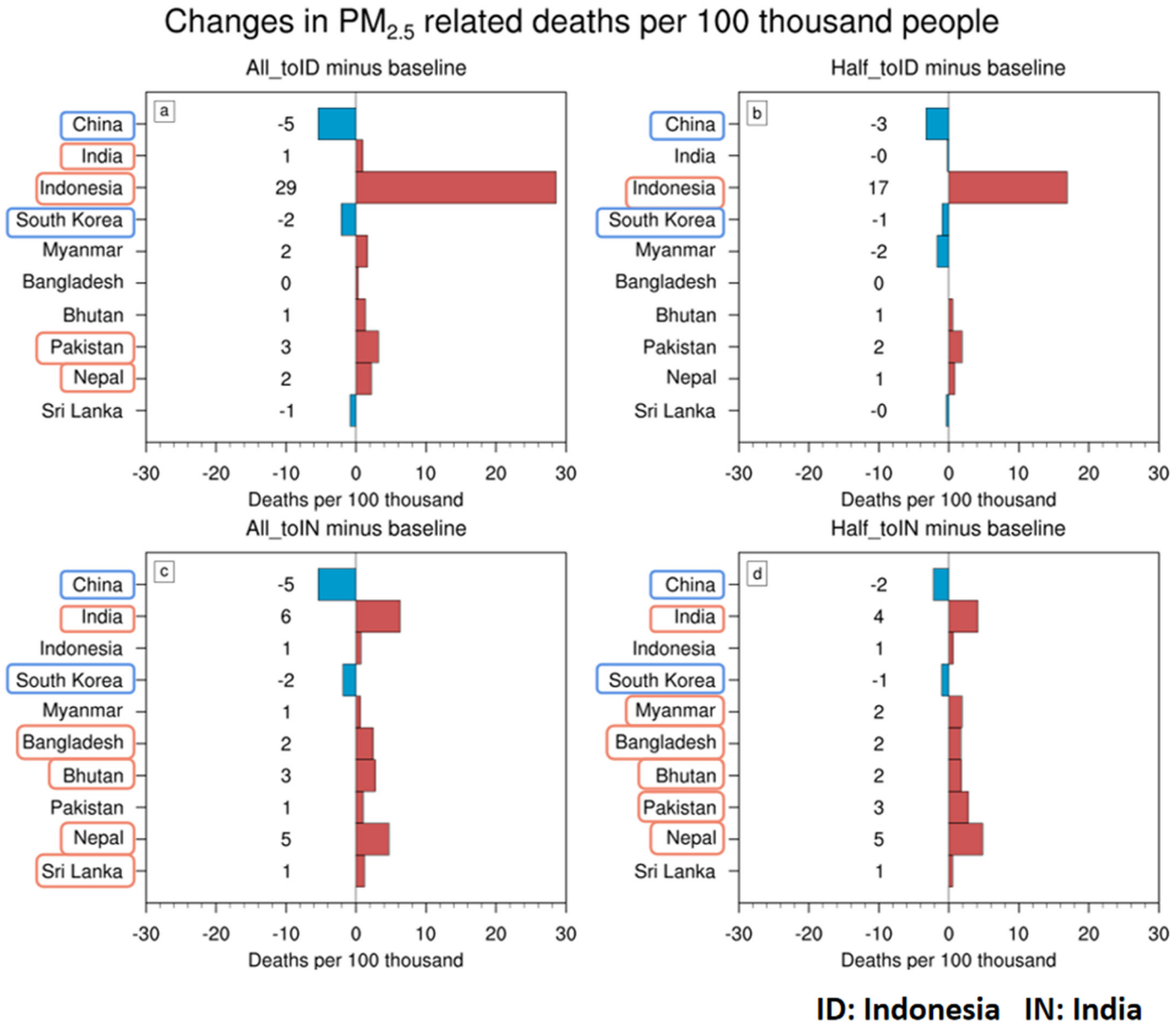

Fig. 5. The median value of 100 estimates of changes in yearly $PM_{2.5}$ related deaths per 100,000 people (see Method 2.6) due to (a) half of China's Emissions Embodied in Exports (EEE) transferred to Indonesia, (b) all of China's EEE transferred to Indonesia, (c) half of China's EEE transferred to India, and (d) all of China's EEE transferred to India. Countries boxed in red/blue have statistically significant increases/decreases in mortality under the two-tailed Wilcoxon signed rank test at 0.05 significance level. Total mortality rates for these countries are shown in Fig. S3.3.

and half scenarios likely represents the importance of extremes in the $PM_{2.5}$ distribution, with 100 years of simulations sometimes not being enough to well define the country 95 % confidence intervals. Mortality rates outside the East, South and Southeast Asian region are unaffected in the simulation.

3.3. Economic responses assessment

We estimated economic costs for individual Asian country in 2020 US dollars ($) of attributable mortality for $PM_{2.5}$ in the baseline and sensitivity simulations by applying mortality estimates from Eq. (3.2) (Supplementary tables 7). The economic cost for a region was based on mortality due to $PM_{2.5}$ pollution and its Willingness To Pay (WTP) to reduce mortality. In the baseline, Chinese economic cost for the 1.66 m annual deaths attributed to $PM_{2.5}$ pollution was estimated to be the highest in Asia, about $2.86 trillion, followed by India ($0.77 trillion for the 0.99 m annual deaths) and Indonesia ($0.10 trillion for the 78k annual deaths). Our estimates are in reasonable accordance with other estimates (OECD Statistics, 2020; Supplementary tables 7) for most of the regions with significant changes in economic cost, but Bangladesh, Bhutan, Myanmar and Nepal are severely overestimated.

To evaluate the economic impact when China's export-related production lines were transferred to India or Indonesia, we subtracted the baseline economic cost from that in the sensitivity simulations (Fig. 6 and Supplementary tables 7). As changes in economic costs attributed to $PM_{2.5}$ related mortality were insignificant outside Asia (Supplementary tables 7), we only focus on the most impacted regions (East, Southeast and South Asia), to analyze the potential economic impact due to manufacturing shift.

When all or half of China's export-related production lines were moved to Indonesia (scenario All_toID and Half_toID), China had the biggest drop in economic cost by $134.6 billion (corresponding to 0.9 % of GDP) and $80.8 billion (corresponding to 0.6 % of GDP) respectively. South Korea also showed significant cost decreases by $3.8 billion in All_toID and $1.7 billion in Half_toID. Indonesia saw the most significant increase in costs, by $96.7 billion or 9.4 % of GDP in All_toID, and by $57.3 billion or 5.6

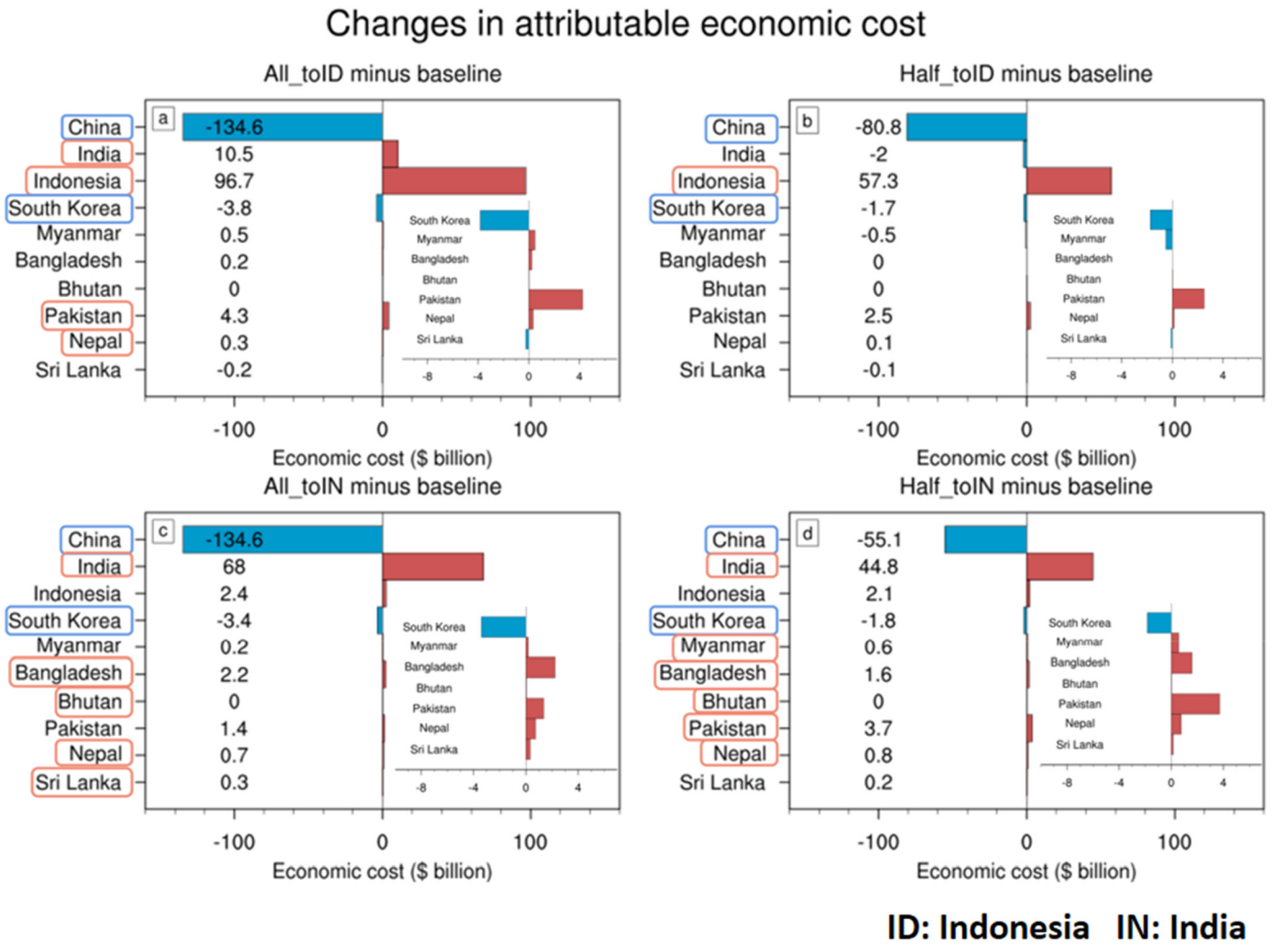

Fig. 6. The median value of 100 estimates of changes in economic cost of $PM_{2.5}$ related deaths ($ billion) due to (a) half of China's Emissions Embodied in Exports (EEE) transferred to Indonesia, (b) all of China's EEE transferred to Indonesia, (c) half of China's EEE transferred to India, and (d) all of China's EEE transferred to India. Countries in red/blue box have statistically significant increases/decreases in economic cost under the two-tailed Wilcoxon signed rank test at 0.05 significance level.

% of GDP in Half_toID. However, costs of other Southeast Asian countries also showed insignificant changes when shifting manufacturing to Indonesia. For South Asia, there would be significant cost increases in India, Pakistan and Nepal, by $10.5 billion, $4.3 billion and $0.3 billion respectively if all of production lines were transferred to Indonesia.

When all of China's export-related production lines were introduced to India (scenario All_toIN), decreases in economic cost of East Asia were more significant than that in Half_toIN. The biggest decreases occurred in China, and the same as for the All_toID scenario, followed by South Korea with cost declines by $3.4 billion. Changes in the economic costs of South Asia are obvious both in the All_toIN and the Half_toIN simulations. Significant increases were simulated in India's annual costs by $68 billion (or 2.7 % of GDP in 2020) and $44.8 billion (or 1.8 % of GDP in 2020) in All_toIN and Half_toIN respectively, as well as to Bangladesh ($2.2 billion and $1.6 billion), and Nepal ($0.7 billion and $0.8 billion). The economic cost to Pakistan increases significantly by $3.7billion in Half_IN, while that to Sri Lanka rose significantly in All_toIN (by $0.3 billion).

Our findings indicated that transferring production lines from China to India or Indonesia contributed to a significant decline in China's attributable economic cost for $PM_{2.5}$ related mortality, and a considerable increase in India or Indonesia's cost. Although the total deaths in India (87.9k) are more than that in Indonesia (73.7k) when transferring comparable production, the VSL of India (0.774) is much smaller than the VSL of Indonesia (1.312). Therefore, the economic cost to India is smaller than that to Indonesia. Furthermore, economic costs of other countries were produced as may be expected from the changed $PM_{2.5}$ attributable deaths. Shifting manufacturing to India impacts more countries than shifting to Indonesia. But simulating half of production lines to Indonesia produced the least significant changes.

Besides the effects on attributable economic costs for $PM_{2.5}$ related mortality, the shift of manufacturing is expected to bring considerable economic benefits to India or Indonesia, as additional production lines can boost local productivity and national GDP. India's CO_2 emissions per GDP is the highest, at 0.91 kg/$, follows by China and Indonesia, at 0.71 and 0.55 kg/$ respectively. In other words, given the same increase in GDP, Indonesia emits the least CO_2 while India emits the most. When all or half of China's export-related production lines were transferred to India, India's GDP increased by $2091 billion or $1045 billion, corresponding to 84.3 % or 42.1 % of GDP in 2020 (World Bank, 2020), which would be much bigger than India's economic cost due to $PM_{2.5}$ related mortality (corresponding to 2.7 % or 1.8 % of GDP). Moving all or half of production lines to Indonesia brought an increase by $3460 billion or $1730 billion in Indonesian GDP, which corresponded to 337 % or 168 % of GDP, far outpacing Indonesia's economic cost (corresponding to 9.4 % or 5.6 % of GDP). However, China's GDP declined by $2680 billion if all of export-related production lines leave, corresponding to 18.3 % of GDP in 2020, which was also much bigger than China's $PM_{2.5}$ attributable economic costs corresponding to 0.9 % of GDP. Cost reduction of China was smaller

in Half_toIN than Half_toID, but they were both much smaller than reductions in China's GDP.

4. Discussion and conclusion

The COVID-19 pandemic is reshaping the global trade and supply chains, and some developed countries may consider relocating strategic manufacturing operations out of China, providing new opportunities for some South and Southeast Asian countries. Since the shift of manufacturing is accompanied by redistribution of emission sources of greenhouse gases and aerosols, the impacts on environment and health of the countries directly involved and their neighbors, should also be considered. Since greenhouse gases are well-mixed in the atmosphere, changes in their emission sources have little impact on climate and the environment. Therefore, we only considered changes in $PM_{2.5}$ concentrations due to aerosols and their precursors. We used the Community Earth System Model version 1.2.2 to simulate $PM_{2.5}$ and the socio-economic responses to very large shifts in economic activity. These huge industrial changes and their associated aerosol and their precursor emissions provide sensitivity studies rather than realistic economic scenarios. In fact, it is difficult to quantify the precise changes of emissions worldwide in the process of manufacturing shift.

Our results indicated that transferring all or half of export production lines from China to India or Indonesia can significantly affect mortality and economic cost attributed to $PM_{2.5}$ changes, especially in China, India and Indonesia, but also in the wider Asian region, especially in the countries downwind of China, Indonesia and India. Shifting manufacturing to India in our simulations led to more Asian countries showing significant changes in $PM_{2.5}$ related deaths and economic costs than an equivalent shift to Indonesia. However, the economic costs of China, Indonesia and India were much smaller than changes in economic benefits due to manufacturing shift. This is of course not the situation for neighboring countries that gain no economic benefit domestically, but suffer (or benefit) from the $PM_{2.5}$ transport.

In making the mortality estimates, the simple 100-year annual mean surface $PM_{2.5}$ concentrations from the climate model do not fit well to satellite observations, particularly in parts of northern China, northern India and Indonesia, the key areas that we focused on. Since the health impacts of $PM_{2.5}$ scale are non-linearly with concentration, a correction for $PM_{2.5}$ in Asia needed to be done rather than work with simple anomalies in $PM_{2.5}$ relative to the baseline.

The range of $PM_{2.5}$ related mortality (Fig. 5) in this study was only determined by uncertainties in the CESM-simulated $PM_{2.5}$ concentrations over the 100-year simulations (in the climate equilibrium state) of the present, and so represents the climate model variability in weather and climate. Although we quote 2.5 % and 97.5 % percentiles of the distribution of 100 estimates as the range of mortality rates, there are other uncertainty sources we do not estimate, such as uncertainties inherent in the relationship between $PM_{2.5}$ exposure and the relative risk of mortality. Other models than the IER type we chose have been used previously to evaluate the relative risk to air pollutant concentrations. Of seven different forms of Concentration-Response functions used previously (Cohen et al., 2004; Pope et al., 2009, 2011), Burnett et al. (2014) considered the IER model was a superior predictor of relative risk. Maji et al. (2018) applied an IER and also non-linear power law (NLP; Chowdhury and Dey, 2016) and log-linear (LL; Lelieveld et al., 2013) models to assess $PM_{2.5}$-related mortality for 338 Chinese cities in 2016. China's total attributable mortality was 9.64 million (IER), 1.258 million (LL) and 0.770 million (NPL). These differences are larger than between the sensitivity scenarios we simulated. However, since we focus on the changes in mortality, the consistent methodology should be sufficient to detect regional and country-by-country differences in response. The model resolution for $PM_{2.5}$ and population are also the key factors that can affect the uncertainties of mortality estimates. We interpolated the lower-resolution $PM_{2.5}$ concentrations into the higher-resolution population grid, because industrial emissions of $PM_{2.5}$ are spatially highly variable and closely linked to population.

The economic cost estimates were based on the 100 estimates of $PM_{2.5}$ related mortality. But there are additional uncertainties from such a monetized assessment of attributable mortality for $PM_{2.5}$. Country-specific empirical studies on the WTP are lacking, particularly in low- and middle-income countries (Roman et al., 2012; Giannadaki et al., 2018), and thus increase the uncertainties in the estimation of VSL and economic costs. Country-specific VSL in this work came from OECD Statistics (2020) for the year 2019. However, Maji et al. (2018) criticized such an unreasonably high estimate of economic cost in China where the VSL was about $0.98 million USD for the year 2010 (Giannadaki et al., 2018), they believe province-specific VSL is a better method for evaluation of economic costs caused by $PM_{2.5}$ related mortality in China than country-specific VSL.

This work only considered the potential effects of redistribution of production lines on human health and social economy, but such economic activity may impact regional temperatures and precipitation through the interaction of aerosols and climate, further leading to socio-economic responses. Our analysis shows that, transferring production lines from China to Indonesia would lead to less Asian countries with significant increases in $PM_{2.5}$ related mortality and attributable economic cost than to India. This is because of the maritime Indonesian setting as well as patterns of surface winds. Higher wind standard deviation over the oceans compared with the land (Fig. 1), means that winds disperse $PM_{2.5}$ more widely from Indonesia than India. In the actual manufacturing redistribution, Indonesia may be a more suitable destination for manufacturing shift compared with India, when we consider fewer negative impacts on local and neighboring countries' air quality and attributable mortality for $PM_{2.5}$. However, since the relationship between $PM_{2.5}$ exposure and the relative risk of mortality is nonlinear, detailed simulation of the mortality impacts including those of neighboring countries should be included in an impact assessment of any real-world manufacturing transfers. At present environmental impact assessments are often done at just the local scale when deciding on infrastructure or industrial development, but the larger picture is clearly important at both domestic and international levels.

As local air quality of India or Indonesia will deteriorate due to the imported production lines, the profits from manufacturing redistribution should first be used to improve the local environment, such as upgrading local industries, developing clean energy technology and carrying out effective environmental management policy. However, the most concerning aspect of this study is the damage to “innocent” victims of any manufacturing shifts in third countries that do not see any domestic economic gains. Morally the “polluter-pays” principle should be applied and the countries that gain economically from any change in production should provide compensation. In practice that can be done statistically, but attributing mortality changes to specific manufacturing industry or areas will be very difficult. The supply and demand shocks caused by COVID-19 are forcing manufacturers worldwide to reassess their supply chains, leading to a growing trend of manufacturing redistribution around the world. Considering the international transport of air pollutants, we believe the “polluter-pay” principle can be applied in current global manufacturing distribution. This is not a study of the health and economic impacts implied by the COVID-19 pandemic, but rather a study of the potential responses to that might be stimulated by unexpected sudden global or regional economic events. While this study can be seen as a purely hypothetical sensitivity study, it is also of interest given the global redistribution of manufacturing towards the global South.

CRediT authorship contribution statement

Qi Ran: Conceptualization, Methodology, Software, Formal analysis, Writing – original draft. **Shao-Yi Lee:** Conceptualization, Methodology, Writing – review & editing. **Duofan Zheng:** Software. **Han Chen:** Resources. **Shili Yang:** Investigation. **John C. Moore:** Conceptualization, Methodology, Writing – review & editing. **Wenjie Dong:** Supervision, Funding acquisition.

Data availability

The atmospheric GHGs concentrations of year 2020 come from NOAA (available at https://gml.noaa.gov/ccgg/trends/). The air pollutant emission inventory comes from CESM1.2 and emissions input fields used to drive the simulations are downloaded automatically during the model building process. Model results shown in this paper are available online (https://doi.org/10.5281/zenodo.6415030).

The satellite-derived $PM_{2.5}$ for assessing model results is available at https://sites.wustl.edu/acag/datasets/surface-pm2-5/. The global gridded population data set is available at https://sedac.ciesin.columbia.edu/data/set/gpw-v4-population-count-rev11. The cause-specific mortalities for the five endpoints (GBD, 2019) are obtained from http://ghdx.healthdata.org/gbd-results-tool. The VSL value for the individual countries or regions is available at https://stats.oecd.org/Index.aspx?DataSetCode=EXP_PM2_5. Carbon dioxide emissions per GDP are available at https://www.climatewatchdata.org/ghg-emissions?calculation=PER_GDP&end_year=2019&regions=CHN,IND,IDN&sectors=total-fossil-fuels-and-cement&source=GCP&start_year=1960. National GDP in 2020 ($ billions, constant 2015; World Bank, 2020) is available at https://data.worldbank.org/indicator/NY.GDP.MKTP.KD.

Declaration of competing interest

The authors declare that they have no known competing financial interests or personal relationships that could have appeared to influence the work reported in this paper.

Acknowledgments

This study was supported by the National Natural Science Foundation of China (U21A6001) and National Natural Science Foundation of China (42075044). The CESM project is supported primarily by the National Science Foundation. The authors thank all the scientists, software engineers, and administrators who contributed to the development of CESM 1.2.

Code availability statement

The code for the CESM 1.2 is publicly available at https://www.cesm.ucar.edu/models/cesm1.2/. The code for post-processing and figure creation is available on request from the corresponding author.

Appendix A. Supplementary data

Supplementary data to this article can be found online at https://doi.org/10.1016/j.scitotenv.2022.158634.

References

Andrew, R.M., 2020. Timely estimates of India's annual and monthly fossil CO2 emissions. Earth Syst. Sci. Data 12 (4), 2411–2421. https://doi.org/10.5194/essd-12-2411-2020.

Apte, J.S., Marshall, J.D., Cohen, A.J., Brauer, M., 2015. Addressing global mortality from ambient PM2.5. Environ. Sci. Technol. 49 (13), 8057–8066. https://doi.org/10.1021/acs.est.5b01236.

BP, 2020. Statistical Review of World Energy [Dataset]. https://www.bp.com/en/global/corporate/energy-economics/statistical-review-of-world-energy.html.

Braathen, N.A., Lindhjem, H., Navrud, S., Directorate, E., Pöyry, E., 2009. Valuing Lives Saved From Environmental, Transport and Health Policies: A Meta-analysis of Stated Preference Studies.

Brauer, M., Freedman, G., Frostad, J., van Donkelaar, A., Martin, R.V., Dentener, F., et al., 2016. Ambient air pollution exposure estimation for the global burden of disease 2013. Environ. Sci. Technol. 50 (1), 79–88. https://doi.org/10.1021/acs.est.5b03709.

Burnett, R.T., Pope 3rd, C.A., Ezzati, M., Olives, C., Lim, S.S., Mehta, S., et al., 2014. An integrated risk function for estimating the global burden of disease attributable to ambient fine particulate matter exposure. Environ. Health Perspect. 122, 397–403. https://doi.org/10.1289/ehp.1307049.

Center for International Earth Science Information Network - CIESIN - Columbia University, 2018. Gridded Population of the World, Version 4 (GPWv4): Population Count, Revision 11 [Dataset]. NASA Socioeconomic Data and Applications Center (SEDAC), Palisades, NY https://doi.org/10.7927/H4JW8BX5.

Chowdhury, S., Dey, S., 2016. Cause-specific premature death from ambient PM2.5 exposure in India: estimate adjusted for baseline mortality. Environ. Int. 91, 283–290. https://doi.org/10.1016/j.envint.2016.03.004.

Cohen, A.J., Anderson, H.R., Ostro, B., Pandey, K.D., Krzyzanowski, M., Künzli, N., et al., 2004. Urban air pollution. In: Ezzati, M., Lopez, A.D., Rodgers, A., Murray, C.J.L. (Eds.), Comparative Quantification of Health Risks: Global and Regional Burden of Disease Attributable to Selected Major Risk Factors. World Health Organization, Geneva, pp. 1353–1434.

van Donkelaar, A., Hammer, M.S., Bindle, L., Brauer, M., Brook, J.R., Garay, M.J., et al., 2021. Monthly global estimates of fine particulate matter and their uncertainty. Environ. Sci. Technol. 55 (22), 15287–15300. https://doi.org/10.1021/acs.est.1c05309.

Fernandes, N., 2020. Economic effects of coronavirus outbreak (COVID-19) on the world economy. IESE Business School Working Paper No. WP-1240-E https://doi.org/10.2139/ssrn.3557504.

Free, C., Hecimovic, A., 2021. Global supply chains after COVID-19: the end of the road for neoliberal globalisation? Account. Audit. Account. J. 34 (1), 58–84. https://doi.org/10.1108/AAAJ-06-2020-4634.

GBD, 2019. Global Burden of Disease Study 2019 Results [Dataset]. Institute for Health Metrics and Evaluation, Seattle, United States. http://ghdx.healthdata.org/gbd-results-tool.

Giannadaki, D., Lelieveld, J., Pozzer, A., 2016. Implementing the US air quality standard for PM2.5 worldwide can prevent millions of premature deaths per year. Environ. Health 15 (1), 88. https://doi.org/10.1186/s12940-016-0170-8.

Giannadaki, D., Giannakis, E., Pozzer, A., Lelieveld, J., 2018. Estimating health and economic benefits of reductions in air pollution from agriculture. Sci. Total Environ. 622–623, 1304–1316. https://doi.org/10.1016/j.scitotenv.2017.12.064.

Global Burden of Disease Collaborative Network, 2013. Global Burden of Disease Study 2010 (GBD 2010) - Ambient Air Pollution Risk Model 1990 – 2010 [Dataset]. Institute for Health Metrics and Evaluation (IHME), Seattle, United States of America. https://doi.org/10.6069/H0RR-H438.

Global Modeling and Assimilation Office (GMAO), 2015. MERRA-2 tavgM_2d_aer_Nx: 2d, Monthly Mean, Time-averaged, Single-level, Assimilation, Aerosol Diagnostics V5.12.4 [Dataset]. Goddard Earth Sciences Data and Information Services Center (GES DISC), Greenbelt, MD, USA. https://doi.org/10.5067/FH9A0MLJPC7N.

Guan, D., Wang, D., Hallegatte, S., Davis, S.J., Huo, J., Li, S., et al., 2020. Global supply-chain effects of COVID-19 control measures. Nat. Hum. Behav. 4, 577–587. https://doi.org/10.1038/s41562-020-0896-8.

Hayakawa, K., Mukunoki, H., 2021. Impacts of COVID-19 on global value chains. Dev. Econ. 59, 154–177. https://doi.org/10.1111/deve.12275.

Hedwall, M., 2020. The ongoing impact of COVID-19 on global supply chains. World Economic Forum. https://www.weforum.org/agenda/2020/06/ongoing-impact-covid-19-global-supply-chains/.

Hurrell, J.W., Holland, M.M., Gent, P.R., Ghan, S., Kay, J.E., Kushner, P.J., et al., 2013. The community earth system model: a framework for collaborative research. Bull. Am. Meteorol. Soc. 94 (9), 1339–1360. https://doi.org/10.1175/BAMS-D-12-00121.1.

IPCC, 2014. In: Pachauri, R.K., Meyer, L.A. (Eds.), Climate Change 2014: Synthesis Report. Contribution of Working Groups I, II and III to the Fifth Assessment Report of the Intergovernmental Panel on Climate Change. IPCC, Geneva, Switzerland, p. 151.

Ivanov, D., 2020. Predicting the impacts of epidemic outbreaks on global supply chains: a simulation-based analysis on the coronavirus outbreak (COVID-19/SARS-CoV-2) case. Transport Res E-Log 136. https://doi.org/10.1016/j.tre.2020.101922.

Lelieveld, J., Barlas, C., Giannadaki, D., Pozzer, A., 2013. Model calculated global, regional and megacity premature mortality due to air pollution. Atmos. Chem. Phys. 13, 7023–7037. https://doi.org/10.5194/acp-13-7023-2013.

Lin, J., Lanng, C., 2020. Here's how global supply chains will change after COVID-19. World Economic Forum. https://www.weforum.org/agenda/2020/05/this-is-what-global-supply-chains-will-look-like-after-covid-19/.

Lin, J., Pan, D., Davis, S.J., Zhang, Q., He, K., Wang, C., et al., 2014. China's international trade and air pollution in the United States. Proc. Natl. Acad. Sci. U. S. A. 111 (5), 1736–1741. https://doi.org/10.1073/pnas.1312860111.

Lin, J., Tong, D., Davis, S., Ni, R., Tan, X., Pan, D., et al., 2016. Global climate forcing of aerosols embodied in international trade. Nat. Geosci. 9, 790–794. https://doi.org/10.1038/ngeo2798.

Liu, X., Easter, R.C., Ghan, S.J., Zaveri, R., Rasch, P., Shi, X., et al., 2012. Toward a minimal representation of aerosols in climate models: description and evaluation in the community atmosphere model CAM5. Geosci. Model Dev. 5, 709–739. https://doi.org/10.5194/gmd-5-709-2012.

Liu, Y., Lee, J.M., Lee, C., 2020. The challenges and opportunities of a global health crisis: the management and business implications of COVID-19 from an Asian perspective. Asian Bus. Manag. 19 (3), 277–297. https://doi.org/10.1057/s41291-020-00119-x.

Lu, X., Lin, C., Li, Y., Yao, T., Fung, J.C., Lau, A.K., 2017. Assessment of health burden caused by particulate matter in southern China using high-resolution satellite observation. Environ. Int. 98, 160–170. https://doi.org/10.1016/j.envint.2016.11.002.

Maji, K.J., Ye, W.F., Arora, M., Shiva Nagendra, S.M., 2018. PM2.5-related health and economic loss assessment for 338 Chinese cities. Environ. Int. 121, 392–403. https://doi.org/10.1016/j.envint.2018.09.024.

Moss, R.H., Edmonds, J.A., Hibbard, K.A., Manning, M.R., Rose, S.K., van Vuuren, D.P., et al., 2010. The next generation of scenarios for climate change research and assessment. Nature 463, 747–756. https://doi.org/10.1038/nature08823.

NBSC, 2017. China Statistical Yearbook 2017 [Dataset]. National Bureau of Statistical of China. http://www.stats.gov.cn/tjsj/ndsj/2017/indexeh.htm.

Neale, R.B., Gettelman, A., Park, S., Conley, A.J., Kinnison, D., Marsh, D., et al., 2012. Description of the NCAR community atmosphere model (CAM 5.0). NCAR Technical Note NCAR/TN-486+STR.

Nicola, M., Alsafi, Z., Sohrabi, C., Kerwan, A., Al-Jabir, A., Iosifidis, C., et al., 2020. The socio-economic implications of the coronavirus pandemic (COVID-19): a review. Int. J. Surg. (Lond. Engl.) 78, 185–193. https://doi.org/10.1016/j.ijsu.2020.04.018.

OECD, 2012. Mortality Risk Valuation in Environment, Health and Transport Policies. OECD Publishing, Paris. https://doi.org/10.1787/9789264130807-en.
OECD, 2014. The Cost of Air Pollution: Health Impacts of Road Transport. OECD Publishing, Paris. https://doi.org/10.1787/9789264210448-en.
OECD, 2017. The Rising Cost of Ambient Air Pollution Thus Far in the 21st Century: Results From the BRIICS and the OECD Countries. OECD Publishing, Paris. https://doi.org/10.1787/d1b2b844-en.
OECD Statistics, 2020. Mortality, morbidity and welfare cost from exposure to environment-related risks [Dataset]. https://stats.oecd.org/Index.aspx?DataSetCode=EXP_PM2_5.
Pope III, C.A., Burnett, R.T., Krewski, D., Jerrett, M., Shi, Y., Calle, E.E., et al., 2009. Cardiovascular mortality and exposure to fine particulate matter from air pollution and cigarette smoke: shape of the exposure-response relationship. Circulation 120, 941–948. https://doi.org/10.1161/CIRCULATIONAHA.109.857888.
Pope III, C.A., Burnett, R.T., Turner, M.C., Cohen, A., Krewski, D., Jerrett, M., et al., 2011. Lung cancer and cardiovascular disease mortality associated with particulate matter exposure from ambient air pollution and cigarette smoke: shape of the exposure–response relationships. Environ. Health Perspect. 119, 1616–1621. https://doi.org/10.1289/ehp.1103639.
Ran, Q., Lee, S.Y., Moore, J.C., Min, C., Dong, W., 2021. Economic shock in a climate scenario and its impact on surface temperatures. Earth's Future 9, e2021EF002061. https://doi.org/10.1029/2021EF002061.
Roman, H.A., Hammitt, J.K., Walsh, T.L., Stieb, D.M., 2012. Expert elicitation of the value per statistical life in an air pollution context. Risk Anal. 32 (12), 2133–2151. https://doi.org/10.1111/j.1539-6924.2012.01826.x.
Sherman, E., 2020. 94% of the Fortune 1000 are seeing coronavirus supply chain disruptions: Report. Fortune. https://fortune.com/2020/02/21/fortune-1000-coronavirus-china-supply-chain-impact/.
Taylor, K.E., Stouffer, R.J., Meehl, G.A., 2012. An overview of CMIP5 and the experiment design. Bull. Am. Meteorol. Soc. 93 (4), 485–498. https://doi.org/10.1175/BAMS-D-11-00094.1.
Textor, C., Schulz, M., Guibert, S., Kinne, S., Balkanski, Y., Bauer, S., et al., 2005. Analysis and quantification of the diversities of aerosol life cycles within AeroCom. Atmos. Chem. Phys. 6, 1777–1813. https://doi.org/10.5194/acp-6-1777-2006.
Wang, Q., Wang, J., He, M.Z., Kinney, P.L., Li, T., 2018. A county-level estimate of PM2.5 related chronic mortality risk in China based on multi-model exposure data. Environ. Int. 110, 105–112. https://doi.org/10.1016/j.envint.2017.10.015.
Wei, T., Dong, W., Moore, J., Yan, Q., Song, Y., Yang, Z., et al., 2016. Quantitative estimation of the climatic effects of carbon transferred by international trade. Sci. Rep. 6, 28046. https://doi.org/10.1038/srep28046.
World Bank, 2020. GDP (constant 2015 US$) [Dataset]. https://data.worldbank.org/indicator/NY.GDP.MKTP.KD.
Zhang, Q., Jiang, X., Tong, D., Davis, S.J., Zhao, H., Geng, G., et al., 2017. Transboundary health impacts of transported global air pollution and international trade. Nature 543, 705–709. https://doi.org/10.1038/nature21712.